第 26 卷第 5 期 无 机 化 学 学 报 Vol.26 No.5
2010 年 5 月 CHINESE JOURNAL OF INORGANIC CHEMISTRY 787-792

# $Zn_3(OH)_2V_2O_7\cdot 2H_2O$ 纳米片的水热制备

曹霄峰 张 雷 马英丽 陈学太*
(南京大学配位化学研究所,配位化学国家重点实验室,南京微结构国家实验室,
南京大学化学化工学院,南京 210093)

**摘要**:采用硝酸锌、五氧化二钒和氢氧化钠作为反应物,通过一个简单的 CTAB 辅助的水热方法制备了 $Zn_3(OH)_2V_2O_7\cdot 2H_2O$ 纳米片。运用 XRD,ICP-AES,FTIR,HRTEM,EDS,FE-SEM 对产物的晶相和形貌进行了表征。结果表明 CTAB 在控制产物的形貌、尺寸分布和自组装过程中起着关键作用。同时我们研究了产物的晶体生长行为和自组装过程。

**关键词**:矾酸盐;锌;自组装;形貌
**中图分类号**:O614.51+1;O614.24+1 **文献标识码**:A **文章编号**:1001-4861(2010)05-0787-06

## Hydrothermal Preparation of $Zn_3(OH)_2V_2O_7\cdot 2H_2O$ Nanodisks

CAO Xiao-Feng ZHANG Lei MA Ying-Li CHEN Xue-Tai*
(*Coordination Chemistry Institute, State Key Laboratory of Coordination Chemistry, Nanjing National Laboratory of Microstructures, School of Chemistry and Chemical Engineering, Nanjing University, Nanjing* 210093)

**Abstract:** $Zn_3(OH)_2V_2O_7\cdot 2H_2O$ nanodisks were prepared by a simple CTAB-assisted hydrothermal route employing the reaction of zinc nitrate, vanadium pentoxide and sodium hydroxide. The phase and morphology of the products were characterized by powder X-ray diffraction (XRD), inductively coupled plasma-atomic emission spectroscopy (ICP-AES), Fourier transform infrared spectroscopy (FTIR), high resolution transmission electron microscopy (HRTEM), energy dispersive X-ray spectroscopy (EDS) and field emission scanning electron microscopy (FE-SEM). The results showed that CTAB played a key role in controlling the morphology, the size and the self-assembly process of the products. The crystal growth behavior and the self-assembly process were also investigated.

**Key words:** vanadate; zinc; self-assembly; morphology

In the past decades transition metal oxides nano/micro-structures have attracted much interest owing to their excellent chemical and physical properties. They are expected to be used in various fields such as information storage, lithium rechargeable batteries, sensors, heterogeneous catalysis, and so on[1-5]. Metal vanadates and their derivatives are an important family of transition metal oxides. Because the vanadium element has a series of variable valence states, it can form various types of oxyacids with different V/O ratio, leading to the versatile metal vanadates including lanthanide-[6-8], bismuth-[9-11], silver-[12-15], iron-[16-17], nickel- or cobalt[18-19], and zinc vanadates[20-22]. In recent years increasing research attention has been paid to zinc vanadates and their derivatives [20-27]. Ye and co-workers[23] have systematically studied photocatalytic activities of $M_3V_2O_8$ (M=Mg, Ni, Zn) in visible-light-driven $O_2$ evolution processes, among which $Zn_3V_2O_8$

收稿日期:2009-10-26。收修改稿日期:2010-01-04。
国家重大基础研究项目(No.2007CB925102)资助。
*通讯联系人。E-mail:xtchen@netra.nju.edu.cn,Tel:025-83597147
第一作者:曹霄峰,男,28 岁,博士研究生;研究方向:纳米材料化学。

showed the highest activity. Zhang et al. [24] have synthesized clew-like $ZnV_2O_4$ hollow spheres and studied the electrochemical properties. Liu et al.[25] have prepared $ZnV_2O_6$ powders by rheological phase reaction and studied their cathodic performance for lithium secondary battery. Bulk $Zn_3(OH)_2V_2O_7\cdot 2H_2O$ was firstly prepared by a hydrothermal process and its crystal structure was determined[26]. It is a layered sandwich-like compound, which adopts a hexagonal lattice [21,26]. The fabrication of the micro- or nano-structured $Zn_3(OH)_2V_2O_7\cdot 2H_2O$ has been rarely reported. Yu and his co-workers[27] have successfully prepared nanosheets of $Zn_3(OH)_2V_2O_7\cdot H_2O$ by a butylamine-assisted hydrothermal procedure. Herein we report the synthesis of $Zn_3(OH)_2V_2O_7\cdot 2H_2O$ nanodisks by a simple surfactant-assisted hydrothermal route at 200 ℃ for 1~18 hours. The role of the surfactant CTAB, the crystal growth behavior and self-assembly process were investigated.

## 1 Experimental

All reagents were purchased from Shanghai Chemical Reagent Corporation and used without further purification. In a typical preparation procedure, $V_2O_5$ (0.001 mol, A.R.), NaOH (0.006 mol, A.R.) and cetyltrimethyl ammonium bromide (CTAB, 2 g, A.R.) were dispersed in 30 mL distilled water under stirring. When these reagents were dissolved, $Zn(NO_3)_2\cdot 6H_2O$ (0.003 mol, A.R.) was added to the resulting colorless solution. Immediately the solution became turbid and viscous. The reaction mixture was stirred at room temperature for 10 minutes and then transferred into a 40 mL Teflon-lined stainless autoclave. The autoclave was sealed and heated at 200 ℃ for 8 h, then allowed to cool to room temperature naturally. The white solid product was collected and separated by centrifugation, washed with distilled water and absolute ethanol several times and finally dried in vacuum at 60 ℃ for 5 hours.

XRD analyses were carried out on a SHIMADZU XRD-6000 powder X-ray diffractometer, equipped with graphite monochromatized Cu $K\alpha$ radiation ($\lambda$= 0.154 18 nm), employing a scanning rate of 4.000 0°·$min^{-1}$, in the $2\theta$ range from 10° to 70°. The operation voltage and current were maintained at 40 kV and 30 mA, respectively. The Zn/V ratio was measured on J-A1100 inductively coupled plasma-atomic emission spectroscopy (ICP-AES). SEM images and EDS were measured on a field emission scanning electron microanalyser Hitachi S-4800 employing an operating voltage of 5 kV or 25 kV. HRTEM images were obtained on a JEM-200CX transmission electronic microscope, employing an accelerating voltage of 200 kV. The FTIR spectrum was recorded between 4 000 and 400 $cm^{-1}$ with a Bruker VECTOR-22 instrument.

## 2 Results and discussion

Fig.1a shows the XRD pattern of the product prepared in the typical procedure. All of the diffraction peaks can be indexed to the hexagonal phase of $Zn_3(OH)_2V_2O_7\cdot 2H_2O$ by comparison with the data from PDF No.50-0570. No peaks of any other phases or impurities were detected. The strong and narrow diffra-

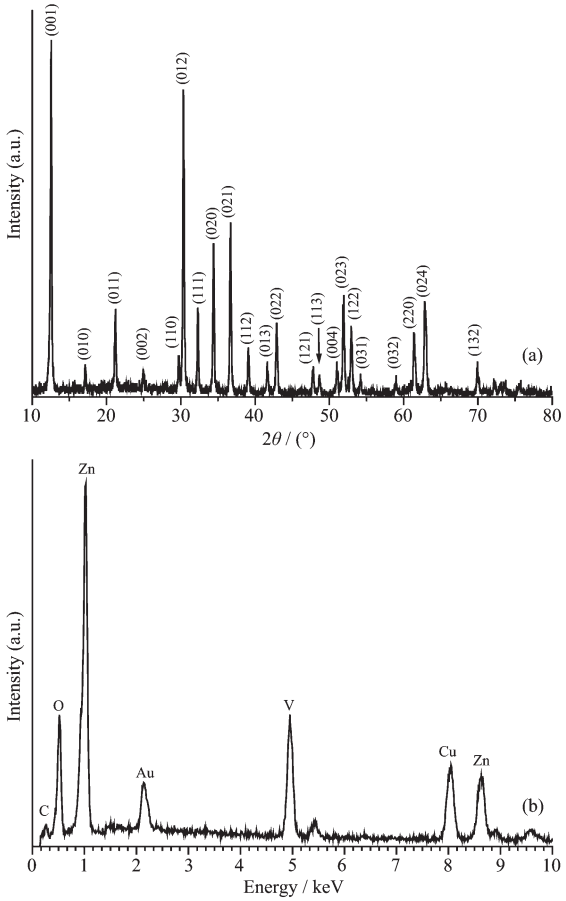


Fig.1 XRD patterns (a) and the EDS spectrum (b) of the product prepared in the typical experiment

ction peaks indicate that the product has good crystallinity. According to the ICP-AES measured data, the Zn/V ratio is 3.00∶1.91, which was in good agreement with the theoretical value. Fig.1b is the EDS spectrum of the typical sample. The peaks of Zn, V, and O can be found. No impurities peaks were detected except Cu, Au and C peaks, which were ascribed to the substrate, the gold plating and $CO_2$ adsorbed by the sample. The $V_2O_7$ group has the characteristic peaks in the FTIR spectrum (Fig.2), which was in agreement with the reported data[28]. Two strong absorption peaks at 907 and 502 $cm^{-1}$ were assigned to $\nu_s$ V (T)-O-Zn (O) and $\nu_s$ V(T)-O-V(T). The letters T and O stand for the tetrahedral and octahedral coordination. The intense absorption peak at 811 $cm^{-1}$ can be ascribed to the corresponding asymmetric vibrations $\nu_{as}$ V (T)-O-Zn(O) and $\nu_{as}$ V(T)-O-V(T). A strong absorption peak at 3 534 $cm^{-1}$ and a medium one at 1 616 $cm^{-1}$ can be assigned to the symmetric stretching vibration and bending vibration of H-O-H in $H_2O$ molecules, respectively. The other strong and broad peak at 3 081 $cm^{-1}$ can be ascribed to the OH group in the framework[28-29]. Two weak absorption peaks at 2 918 $cm^{-1}$ and 2 849 $cm^{-1}$ may be attributed to the symmetric and asymmetric stretching vibration of $CTA^+$[29].

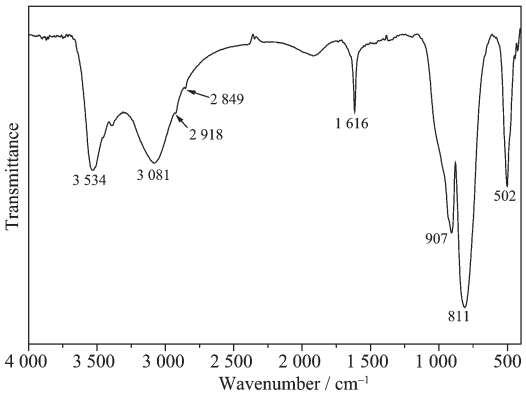


Fig.2　FTIR spectra of the sample prepared in the typical experiment

Fig.3a is the low-magnification FE-SEM image of the sample obtained in the typical procedure, indicating that the product was $Zn_3(OH)_2V_2O_7\cdot 2H_2O$ nanodisks with the average thickness of 90 nm, which was further proved by the typical high-magnification FE-SEM and TEM images (Fig.3b and 3c). Furthermore, most of the nanodisks were self-assemblied into layer-by-layer microstructures.

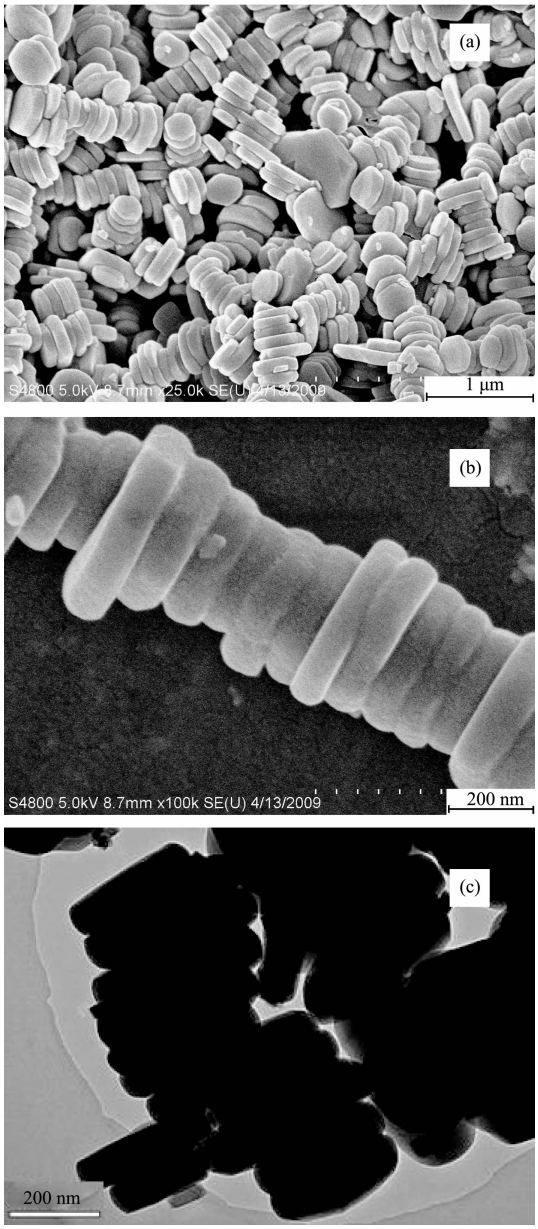


Fig.3　FE-SEM and TEM images of the sample prepared in the typical experiment

CTAB has been widely used as a capping agent and/or a soft template to arrange nanomaterials to form the ordered structures[30-36]. In order to investigate the effect of CTAB on the morphology and size of the product, some controlled experiments were carried out under the same conditions except different amounts of CTAB. Fig.4a is the FE-SEM image of the product prepared in the absence of CTAB, which shows that the sample was nano/sub-micro particles with the irregular

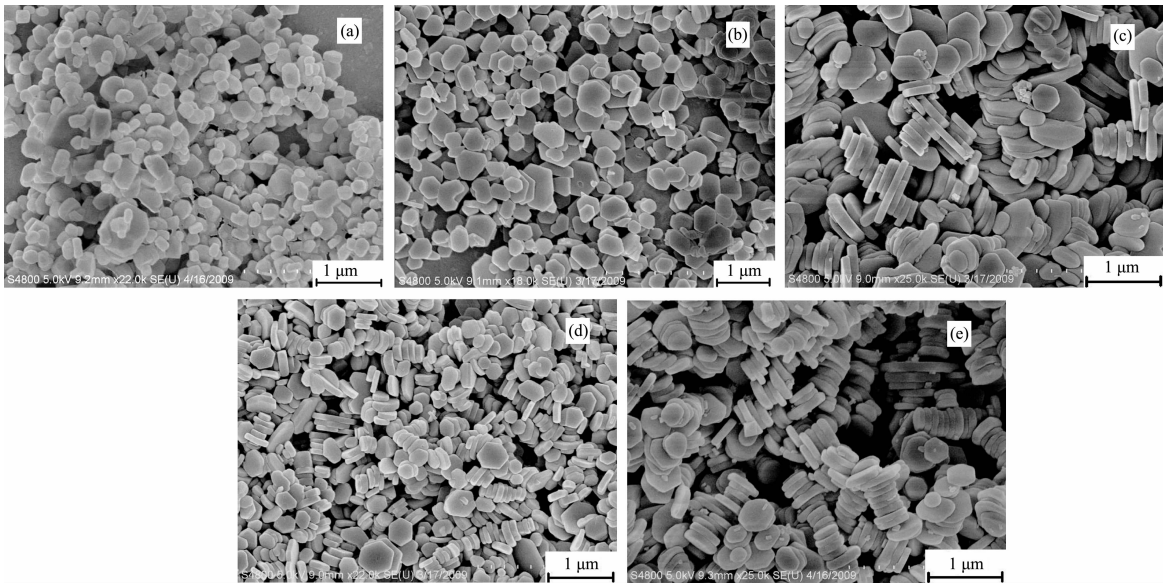


(a) 0 g, (b) 0.1 g, (c) 0.5 g, (d) 1 g, and (e) 3 g

Fig.4 FE-SEM images of the products prepared with different amount of CTAB

morphology and wide size distribution. This observation indicated that CTAB played a key factor in controlling the morphology and size distribution and self-assembly process. When 0.1 g CTAB was used, the morphology of the product was the nanodisks with the average thickness from 80 to 90 nm and few self-assembled units were formed (Fig.4b). When the amount of CTAB was increased to 0.5 g or 1 g (Fig.4c, 4d), the percentage of the self-assembled units increased obviously. With 2~3 g of CTAB was used, the product had the best size distribution and most nanodisks were arranged to form layer-by-layer self-assembled structures (Fig.3, 4e).

The reaction temperature can greatly influence the chemical reaction process and the morphology of the products. Reducing the reaction temperature to 180 ℃ (Fig.5a), the average thickness of the nanodisks decreased to about 60 nm and the percentage of the self-assembled structures decreased. With the further decrease of the reaction temperature to 140 ℃ and 100 ℃, the hexagonal nanodisks gradually changed to the round disks with the decreasing of the average thickness of 20~30 nm (Fig.5b and c). No obvious self-assembled structures were observed. These observations suggested that the high temperature is favorable for the formation of the layer-by-layer self-assembled structures.

In order to understand the crystal growth behavior and self-assembly process, a series of time-dependent experiments were performed. When the reaction time was 1 h, the nanosheets of $Zn_3(OH)_2V_2O_7\cdot 2H_2O$ with the average thickness of 10~20 nm were formed (Fig.6a). After reaction for 3 h, disk-like particles with thickness of *ca.* 50 nm were formed, among which a few self-

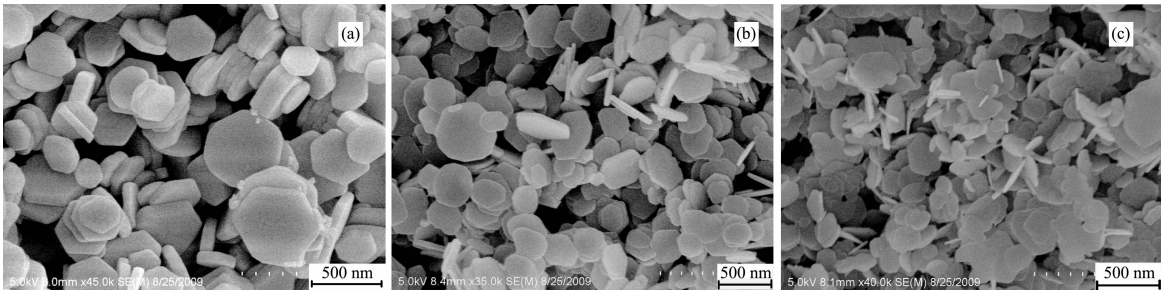


(a) 180 ℃, (b) 140 ℃, and (c) 100 ℃

Fig.5 FE-SEM images of the products prepared at different reaction temperature

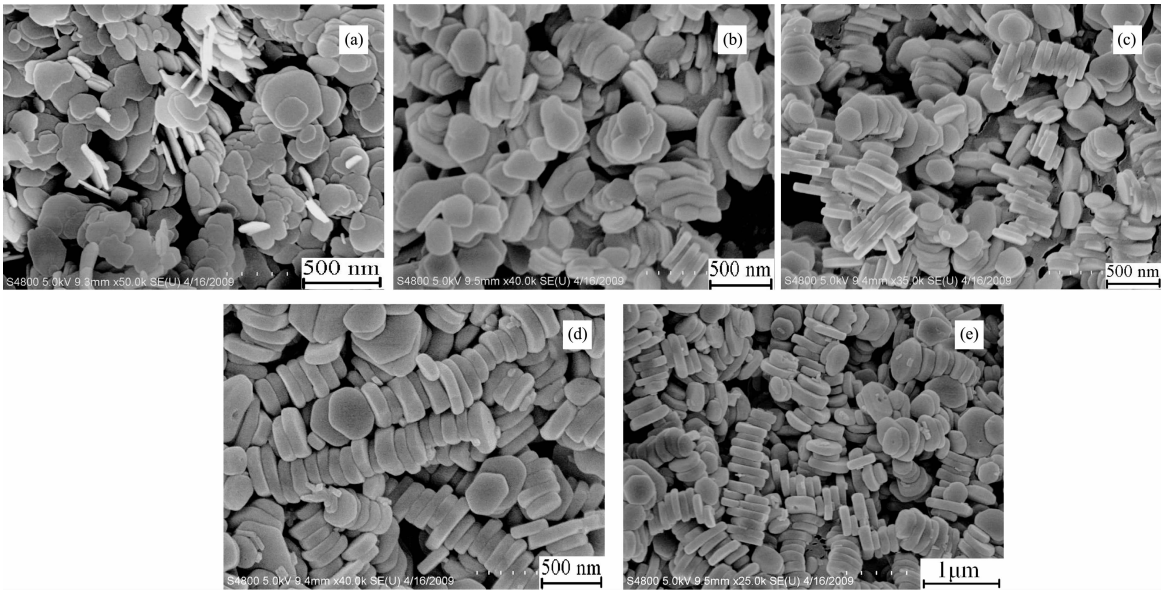


(a) 1 h, (b) 3 h, (c) 5 h, (d) 12 h, and (e) 18 h

Fig.6　FE-SEM images of the products prepared at 200 ℃ for different time

assembled structures appeared (Fig.6b). Further prolonging the reaction time to 5 h, 12 h and 18 h, the thickness of nanodisk gradually increased to about 90 nm and more layer-by-layer self-assembled structures were obtained. Based on these time-dependent experiments, the formation process of layer-by-layer self-assembled structures is schematically illustrated in Fig.7. The formation possibly followed the three steps. The initially formed amorphous $Zn_3(OH)_2V_2O_7\cdot 2H_2O$ become crystallized and then grew into nanosheets via the Ostwald ripening mechanism under hydrothermal conditions because of the layered crystal structure. It is generally believed that materials with hexagonal crystal structures are particularly predisposed to anisotropic growth and hexagonal plates are easily to be formed[37-38]. The van der Waals forces between the hexagonal nanosheets capped by CTAB can impel the nanosheets oriented in an ordered way. CTAB actually serves as a cohesive agent[35]. Once the hexagonal $Zn_3(OH)_2V_2O_7\cdot 2H_2O$ nanosheets were established, they intimately contact each other in a face-by-face manner to form layer-by-layer structures with the assistance of CTAB. Fig.8, the HRTEM images of the product, showed the nanosheets stacked along the (001) direction. It is necessary to point that the assembly process could be reversible and the self-assembly intensity is not monodisperse. Also the individual nanosheet could grow along the thickness direction and became thicker. Other surfactants were also studied and few self-assembled microstructures were formed except polyvinylpyrrolidone.

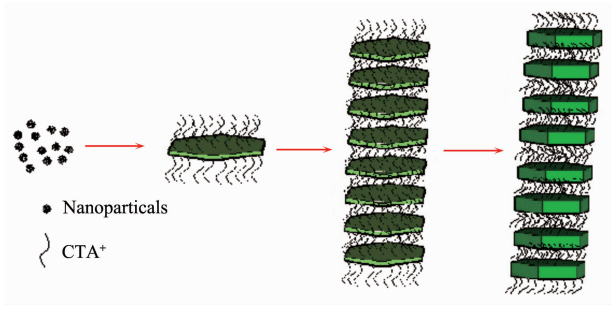


Fig.7　Schematic illustration of formation mechanism of self-assembled structures of $Zn_3(OH)_2V_2O_7\cdot 2H_2O$ nanodisks

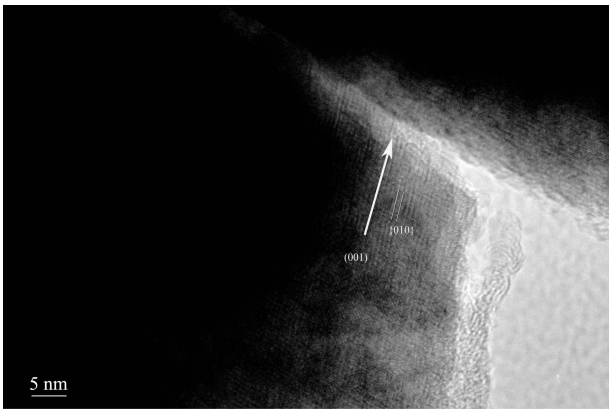


Fig.8　HRTEM image of the product

## 3 Conclusions

In summery, $Zn_3(OH)_2V_2O_7\cdot 2H_2O$ nanodisks were obtained by a simple CTAB-assisted hydrothermal route at 200 ℃ employing zinc nitrate, vanadium pentoxide and sodium hydroxide as reagents. FE-SEM images showed CTAB played an important role in controlling the size, morphology and the process of the crystal growth and self-assembly. The time evolution experiments indicated that the self-assembly might follow a three-step formation mechanism.

## References:


[1] Park J, Kim J, Kwon H, et al. *Adv. Mater.*, **2009**,**21**:803-807

[2] Cao A M, Hu J S, Liang H P, et al. *J. Phys. Chem. B*, **2006**, **110**:15858-15863

[3] Shanmugam S, Gedanken A. *J. Phys. Chem. C*, **2008**,**112**: 15752-15758

[4] Pan Z W, Dai Z R, Wang Z L. *Science*, **2001**,**291**:1947-1949

[5] Qian L W, Zhu J, Chen Z, et al. *Chem. Eur. J.*, **2008**,**15**:1233-1240

[6] Pan G H, Song H W, Bai X, et al. *J. Phys. Chem. C*, **2007**,**111**: 12472-12477

[7] Yu C C, Yu M, Li C X, et al. *Cryst. Growth Des.*, **2009**,**9**:783-791

[8] Yang P P, Quan Z W, Lu L L, et al. *Nanotechnology*, **2007**,**18**: 235703(10pp)

[9] Zhang L, Chen D R, Jiao X L. *J. Phys. Chem. B*, **2006**,**110**: 2668-2673

[10]Strobel R, Metz H J, Pratsinis S E. *Chem. Mater.*, **2008**,**20**: 6346-6351

[11]Zhou L, Wang W Z, Zhang L S, et al. *J. Phys. Chem. C*, **2007**, **111**:13659-13664

[12]Shao M W, Lu L, Wang H, et al. *Chem. Commun.*, **2008**:2310-2312

[13]Mao C J, Wu X C, Pan H C, et al. *Nanotechnology*, **2005**,**16**: 2892-2896

[14]Xiong C R, Aliev A E, Gnade B, et al. *ACS Nano*, **2008**,**2**: 293-301

[15]Song J M, Lin Y Z, Yao H B, et al. *ACS Nano*, **2009**,**3**:653-660

[16]Nivoix V, Gillot B. *Chem. Mater.*, **2000**,**12**:2971-2976

[17]Takei H, Suzuki T, Katsufuji T. *Appl. Phys. Lett.*, **2007**,**91**: 072506(3 pp)

[18]He Z Z, Ueda Y, Itoh M. *J. Cryst. Growth*, **2006**,**297**:1-3

[19]He Z Z, Yamaura J, Ueda Y, et al. *J. Am. Chem. Soc.*, **2009**, **131**:7554-7555

[20]Zhang Y, Debord J R D, O′Connor C J, et al. *Angew. Chem. Int. Ed. Engl.*, **1996**,**35**:989-991

[21]Chirayil T, Zavalij P Y, Whittingham M S. *Chem. Mater.*, **1998**,**10**:2629-2640

[22]Skibsted J, Jacobsen C J H, Jakobsen H J. *Inorg. Chem.*, **1998**,**37**:3083-3092

[23]Wang D F, Tang J W, Zou Z G, et al. *Chem. Mater.*, **2005**,**17**: 5177-5182

[24]Xiao L F, Zhao Y Q, Yin J, et al. *Chem. Eur. J.*, **2009**,**15**: 9442-9450

[25]Liu H W, Tang D G. *Mater. Chem. Phys.*, **2009**,**114**:656-659

[26]Zavalij P Y, Zhang F, Whittingham M S. *Acta Crystallogr. C*, **1997**,**53**:1738-1739

[27]Qian H S, Yu S H, Gong J Y, et al. *Cryst. Growth Des.*, **2005**, **5**:935-939

[28]Hoyos D, Palacio L A, Paillaud J L, et al. *Solid State Sci.*, **2004**,**6**:1251-1258

[29]Wu X C, Tao Y R, Song C Y, et al. *J. Phys. Chem. B*, **2006**, **110**:15791-15796

[30]Lin Z H, Chang H T. *Langmuir*, **2008**,**24**:365-367

[31]Song R Q, Xu A W, Yu S H. *J. Am. Chem. Soc.*, **2007**,**129**: 4152-4153

[32]Surendran G, Ramos L, Pansu B, et al. *Chem. Mater.*, **2007**, **19**:5045-5048

[33]Nakanishi H, Tsuchiya K, Okubo T, et al. *Langmuir*, **2007**, **23**:345-347

[34]Cao M H, Hu C W, Wang Y H, et al. *Chem. Commun.*, **2003**: 1884-1885

[35]Guo L F, Murphy C J. *Nano Lett.*, **2003**,**3**:231-234

[36]Mi Y, Huang Z Y, Hu F L, et al. *J. Phys. Chem. C*, **2009**,**113**: 20795-20799

[37]Du W M, Qian X F, Ma X D, et al. *Chem. Eur. J.*, **2007**,**13**: 3241-3247

[38]DU Wei-Min(杜卫民). *Thesis for the Doctorate of Shanghai Jiao Tong University*(上海交通大学博士论文). **2007**.